Korean J. Chem. Eng., 37(3), 497-504 (2020)
DOI: 10.1007/s11814-019-0436-2

pISSN: 0256-1115
eISSN: 1975-7220

Preparation and antifouling performance of PVDF-DCOIT composite hollow fiber membranes

Sen Qiao†, Hongjie Cao, Yue Yang, Ruofei Jin, and Jiti Zhou

Key Laboratory of Industrial Ecology and Environmental Engineering (Ministry of Education, China), School of Environmental Science and Technology, Dalian University of Technology, Dalian 116024, P. R. China
(*Received 21 June 2019 • accepted 21 November 2019*)

Abstract−Membrane fouling is the main bottleneck that hinders the applications of membrane bioreactors (MBRs). 4,5-Dichloro-2-n-octyl-4-isothiazolin-3-one (DCOIT), as an environmentally-acceptable antifouling biocide, was mixed with Polyvinylidene fluoride (PVDF) to fabricate hollow fiber membrane via non-solvent induced phase separation (NIPS), which was able to effectively improve the antifouling performance of the membranes in this work. Overall research of the prepared membrane revealed that membranes with 3 wt% DCOIT exhibited the optimum antifouling performance. With the addition of DCOIT, hydrophilicity and pure water flux of 3 wt% DCOIT membranes maintained remarkable improvement by 22.9% and 64.6% than that of membranes without DCOIT. Meanwhile, the surface morphologies of 3 wt% DCOIT membranes were smoother than the control group in terms of SEM and AFM images, which was beneficial to alleviate membrane fouling. In antifouling experiments, the flux variation rate of membranes with 3 wt% DCOIT filtrated in bull serum albumin, sodium alginate and humic acid solution were 81.42%, 54.25%, 50.5%, while membrane without DCOIT were 64.6%, 24.72% and 29%, respectively. Similar results were obtained by filtrating anaerobic sludge for 24 h. The flux variations of 3 wt% DCOIT membranes were 59.4%, 47.8% and 46.0%, respectively in three stages. However, the flux variations of membranes without DCOIT were 44.8%, 36.7% and 19.8%, respectively, which showed better antifouling ability and higher flux recovery efficiency. The novel membranes would provide some theoretical basis and technical support for the rational combinations in elevating the overall antifouling properties of membranes.

Keywords: MBR, PVDF Hollow Fiber Membrane, DCOIT, Antifouling Performance

INTRODUCTION

Membrane bioreactor (MBR) technology for wastewater treatment has received extensive attention and achieved rapid development in practical application for over three decades [1,2]. Compared to conventional treatment processes, MBRs have significant advantages such as better effluent quality, higher sludge loading, less waste sludge production and without worrying about sludge settling, etc [3,4]. Although MBRs have been widely used as a reliable treatment process [5], membrane fouling is the main bottleneck that hinders their applications [6]. There are three main factors which affect the membrane antifouling performance: the nature of the influent, the hydrodynamic environment of membrane and inherent nature of membrane including morphology, charge and hydrophilicity of membrane surface and so on [7]. For wastewater treatment, membrane foulants are mainly resulted from biomacromolecules, humic substances, inorganic salts, bacteria and so on [8]. Many ways had been researched for solving the fouling of membrane surface such as pretreatment of raw water, optimization design and membrane rinse [9]. Even so membrane fouling couldn't be fundamentally eliminated by all methods mentioned above. Developing novel membranes with good antifouling might be an effective strategy. There are a variety of methods explored to prepare new membranes with excellent antifouling properties, for instance, surface modification and blending modification [10]. However, most of the methods aimed to prevent the initial adsorption of foulants on the membrane surface and ignored that their intrinsic features [11] are inherently restricted in bacterial adhesion and colonization [2,12]. Alternative means depends on the effect of antimicrobial agents with the purpose of effectively limiting microbial colonization and suppress biofilm growth [8]. As releasable antimicrobial agents, silver and copper nanoparticles are against a broad-spectrum of microorganisms from Gram-positive to Gram-negative bacterial and microalgae, which could be broadly used for preparing of antifouling membranes [9,13-15]. Nevertheless, these inorganic biocides are difficult to be well dispersed with membrane materials and agglomeration was always observing on the membrane surface, which make the constructure become brittle and reduce its stability.

Sea-Nine211, as a novel marine antifouling agent with the excellent performance, is the alternative of organotin-based antifouling paints. The latter means were banned because of the bio-accumulation and bio-toxicity to non-target organisms [16]. 4,5-Dichloro-2-n-octyl-4-isothiazolin-3-one (DCOIT) is the main active ingredient in the Sea-Nine211 against a wide spectrum of bacteria, fungi and algae [17]. DCOIT has been widely considered as an environmental-friendly antifouling agent due to its high antifouling activity and short environmental half-life [18], which became the first organic biocide registered by US Environmental Protection Agency, and

†To whom correspondence should be addressed.
E-mail: qscyj@mail.dlut.edu.cn

has been awarded the 'Green Chemistry Challenge Award' for its environmental safety [19]. Furthermore, compared to inorganic antimicrobial agents [20], DCOIT could be dispersed evenly with membrane materials without any agglomeration on the surface. Generally, DCOIT has a great potential to be an excellent additive for the preparation of novel membranes with good antifouling performances.

In the present work, polyvinylidene fluoride (PVDF) powder was blended with the biocide DCOIT to fabricate membranes by the conventional non-solvent induced phase separation (NIPS) [9,21]. The effect of DCOIT dosages on the overall performance of the prepared membranes was studied. Besides, the antifouling experiments were carried out in anaerobic bioreactors with the dead-end filtration under the constant transmembrane pressure (TMP) [22]. The improved antifouling performance of membranes would provide some theoretical basis and technical support for the rational combinations in elevating the overall antifouling properties of membranes.

MATERIALS AND METHODS

1. Materials

Polyvinylidene fluoride (PVDF) was bought from Shandong West Asia Chemical Co., Ltd. Aladdin Industrial Corporation supplied antifouling booster biocide 4,5-dichloro-2-n-octyl-4-isothiazolin-3-one (DCOIT). N,N-dimethylformamide (DMF) was bought from Xilong Chemical Company Co., Ltd. Polyvinyl pyrrolidone (PVP) was provided from Guangfu Fine Chemical Research Institute, Tianjin. Humic acid (HA) and bovine serum albumin (BSA) were offered by Sigma Aldrich Chemical Co., Ltd., USA. All chemical reagents used in the research were of analytical grade. Anaerobic sludge was originated from the laboratory-scale bioreactor.

2. Preparation of PVDF-DCOIT Composite Hollow Fiber Membrane

The PVDF-DCOIT composit hollow fiber membrane was fabricated by non-solvent induced phase separation (NIPS) [23-27]. The casting solution consisted of PVDF, PVP and glycerol in DMF as solvent. DCOIT was dispersed and dissolved until forming the homogeneous solution at 45 °C. Component of the casting solution for all membranes was shown in Table 1. The casting solution was directly injected into the non-solvent bath (ultrapure water) by a double-channel microinjector. Hollow fiber membrane was formed via primary phase separation. And then the prepared membrane was placed in fresh distilled water for 24 hours to make sure the complete phase separation. Finally, immersed the membrane into glycerine solution (50/50 wt%) for 24 h and then dried by natural air.

Table 1. The compositions of PVDF membranes in different DCOIT concentrations

Type (wt%)	PVDF	DMF	Glycerol	PVP	DCOIT
Control	12.0	72.0	4.0	12.0	--
S1	12.0	71	4.0	12.0	1
S2	12.0	70	4.0	12.0	2
S3	12.0	69	4.0	12.0	3
S4	12.0	68	4.0	12.0	4

3. Hydrophilicity and Filtration Experiment

Water contact angle was used to evaluate the wetting ability and hydrophilicity of the material surface to water, and the membrane with lower water contact angle was more hydrophilic [23]. In this work, water contact angles of the prepared membranes were measured by automatic contact angle meter (SL200B, Kono Industrial Co., Ltd., USA) at room temperature. Ultrapure water droplets (2 μL) were dripped on the membrane surface. Water contact angle of membrane surface was measured at least 3 different samples of each group.

Permeability of the membranes was presented by their pure water flux. The filtration process was kept steady for at least 30 minutes at the transmembrane pressure (TMP) of 0.1 MPa. The pure water flux [28] was measured by a dead-end filtration device and calculated by Eq. (1):

$$J = \frac{V}{A \cdot \Delta t} \quad (1)$$

where J is the pure water flux (L/m^2·h), V is the volume of the effluent (L), A is the surface area of the membrane modules (m^2) and Δt is the effluent collection interval (h). The measurement result was the average of three testing values at room temperature.

4. Pore Size and Porosity

Mercury intrusion porosimetry (Autopore IV 9510, Micromeriti CS) was to characterize the pore-size distribution and mean pore diameter of the samples. The mean porosity (ε) was determined by the gravimetric method [29]. The mean value was measured at least 5 different samples of each group, as calculated in the following Eq. (2):

$$\varepsilon = \frac{\omega_1 - \omega_2}{A \times l \times d_w} \quad (2)$$

where ω_1 is the weight of the wet membrane; ω_2 is the weight of the dry membrane; A is the surface area of membrane modules (m^2), l is the membrane thickness (m) and d_w is the density of water (998 kg/m^3). Finally, take the average value of three samples as the test results.

5. Morphologies of PVDF-DCOIT Composite Hollow Fiber Membranes

Scanning electron microscope (FESEM, HitachiS-8010) was used to analyze surface morphologies of the prepared membranes. The membrane samples were dried at room temperature and then sputter-coated with gold to provide electrical conductivity. The composition and distribution of chemical elements on the membrane surface were measured by energy dispersive X-ray spectroscopy (EDS).

Surface roughness was measured by the atomic force microscopy (AFM, Bruker Dimension Icon, Germany). The membrane samples were operated in the tapping mode. The surface roughness parameters were represented by average roughness (S_α), the root mean square of the Z data (S_q) and the average deviation in height between highest peaks and the lowest valleys relative to the mean plane (S_z).

6. Antifouling Experiments

The dead-end filtration was carried out with BSA (1 g/L), SA

(1 g/L) and HA (1 g/L) as surrogates for proteins and polysaccharides in wastewater [30]. The prepared membranes were made of modules with an effective filtration area of 30 cm^2. The TMP was kept at 0.08 MPa during permeation of the BSA, SA and HA solution. The flux was measured every 10 min and each test lasted for 1.5 h.

Antifouling experiments against microbial foulants were performed with the dead-end filtration in the anaerobic bioreactors. The prepared membranes were still made of modules with an effective filtration area of 30 cm^2. The TMP was kept at 0.08 MPa during filtration of 1,000 mg/L anaerobic active sludge. The water flux of the prepared membranes was recorded every 2 hours and the hydraulic rinsing was operated for 30 mins after the filtration of 8 hours. The cleaned membrane was used to filtrate the same foulants once again to evaluate the flux recovery for the next running stage. Three stages were carried out for the antifouling tests.

RESULTS AND DISCUSSION

1. Hydrophilicity and Pure Water Flux

A hydrophilic membrane can effectively resist the membrane fouling caused by organic matter and maintain a high flux under the same TMP. Because the hydrophilic membrane can be wetted by water and form water film on the surface of membrane, which can effectively alleviate the adhesion of hydrophobic substance on the membrane surface and significantly mitigate the membrane fouling [23]. As shown in Fig. 1, contact angle was reduced remarkably after the addition of DCOIT into casting solution. Membranes without DCOIT (control group) had the highest water contact angle (82.12°). Water contact angle of the prepared membranes were decreased to 76.25° and 72.05° with the addition of 1 wt% DCOIT (S1) and 2 wt% DCOIT (S2), respectively. And the water contact angle was the lowest (63.35°) when the dosage of DCOIT reached 3 wt%, which was about 1.23 times better than that of membranes without DCOIT. DCOIT mixed into the PVDF materials could effectively increase the hydrophilicity of the membranes.

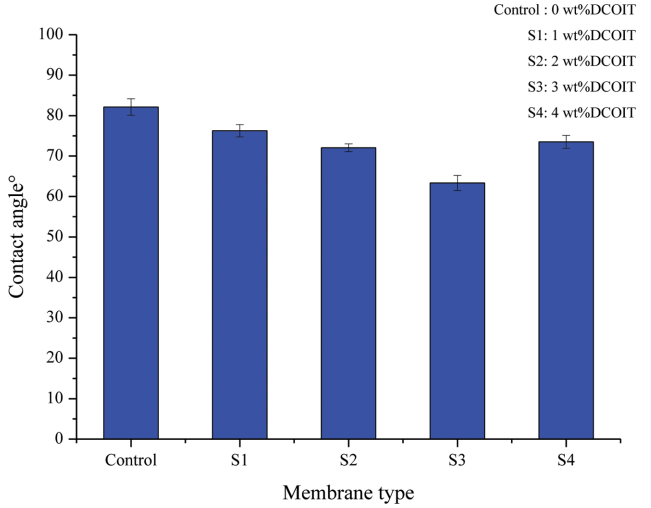

Fig. 1. Effects of different DCOIT contents on the contact angle of the membrane surface.

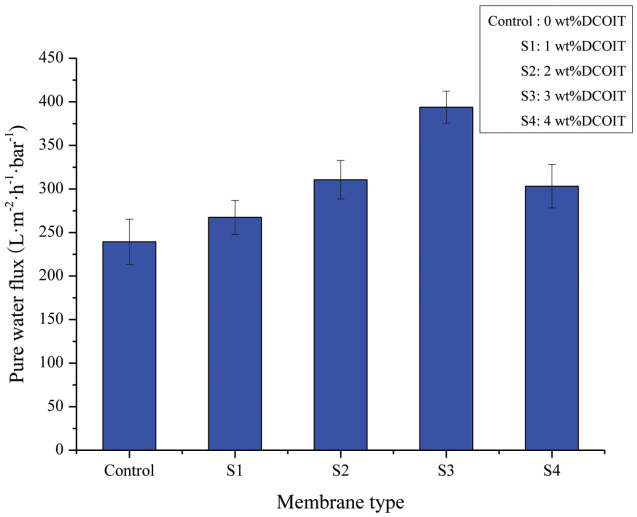

Fig. 2. Effects of different DCOIT contents on pure water flux of the membranes.

Pure water flux is one of the most important parameters for membrane performance to characterize the permeability of water [23]. Fig. 2 indicated that the pure water flux of the prepared membrane was obviously enhanced with the increasing of DCOIT content. And pure water flux of membranes with 3 wt% DCOIT (S3) was the highest (393.86 $L \cdot m^{-2} \cdot h^{-1} \cdot bar^{-1}$), which was improved by 64.6% than that of membrane without DCOIT. But when the DCOIT concentration was up to 4 wt% (S4), the pure water flux and contact angle of membranes were both decreased, since increasing of the solution viscosity hindered the phase-separation rate in the high blending ratio. As a result, finger-like pore structure was restrained in the immersion precipitation process and the performance of membrane was reduced [31]. Therefore, it was preliminarily believed that the membranes blended 3 wt% DCOIT had the best performance among the five groups with the best hydro-

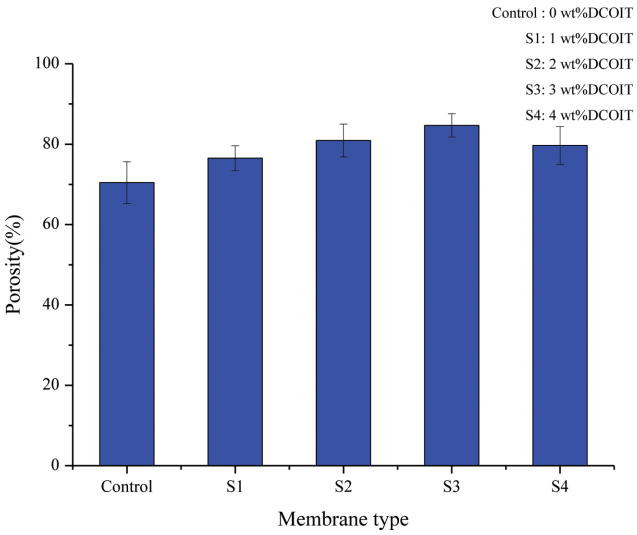

Fig. 3. Effects of different DCOIT contents on overall porosity of the membranes.

philicity and the largest pure water flux.

2. Porosity and Pore Size

Higher porosity and pore size were attributed to resist membrane permeate flux loss during the filtration [23]. As shown in Fig. 3, the porosity of the prepared membranes ranging from S1 to S4 was all improved, which was significantly larger than that of control group (70.4%). Polyvinyl pyrrolidone (PVP), as a pore-forming reagent with good water solubility, separated out from membrane matrix by the exchange of solvent and nonsolvent in the coagulation bath for forming dense finger-like pores under the membrane layer [32], which had an important effect on porosity of the prepared membrane. Meanwhile, the trend of overall porosity was consistent with the water flux and contact angle due to phase separation process influencing the morphology and structure of membrane surface, which was proved in the following discussion of SEM and AFM characteristics. And the membranes with 3 wt% DCOIT had the highest porosity (84.7%), which indicated that DCOIT might accelerated exchanging of the solvent and nonsolvent so as to promote the formation of dense finger-like pores [33]. Fig. 4 depicted that the mean pore size of the membranes was also improved with the increasing DCOIT content and membranes with 3 wt% DCOIT had the largest average pore diameter (0.55 μm), which manifested that DCOIT could promote the formation of larger pores. However, membranes with 4 wt% DCOIT had smaller pore diameter because of high viscosity.

3. Morphologies of PVDF-DCOIT Composite Hollow Fiber Membranes

Smoother surface was attributed to inhabit pollutants depositing on the membrane surface [23]. According to the above results, the overall performance of 3 wt% DCOIT membrane (such as pure water flux, contact angle and porosity, etc.) was significantly better than others. The morphologies of membrane with 3 wt% DCOIT and control group were characterized to further determine the physical and chemical properties of PVDF-DCOIT hollow fiber membrane through microscopic images. Fig. 5(a), (b) showed the surface SEM images of control group and membrane with 3 wt% DCOIT. The surface of 3 wt% DCOIT membrane was relatively smoother than that of membrane without DCOIT, which demonstrated that DCOIT could be mixed evenly with casting solution. And the addition of DCOIT made the membranes had a smoother surface and higher porosity than the membranes without DCOIT. The smooth surface could alleviate the membrane fouling by reducing the adhesion and growth of organic foulants and microbial foulants and extend their application life [6,27]. The cross-sectional SEM images of 0 wt% DCOIT and 3 wt% DCOIT membrane were exhibited in Fig. 5(b), (d), which showed typical characteristics of porous membrane structure with a dense surface layer and a finger-like porous inner layer [34]. The finger-like pores of the membranes with 3 wt% DCOIT were obviously wider and smoother than that of the membranes without DCOIT. The hydrophilicity of DCOIT increased the phase separation between the solvent and the nonsolvent [35], so that formed the larger pore channels. Moreover, these pore channels improved the porosity which increased the flux of the membranes.

The energy dispersive spectrometer (EDS) was used for elemental analysis of the membranes. Element sulfur and chlorine are the

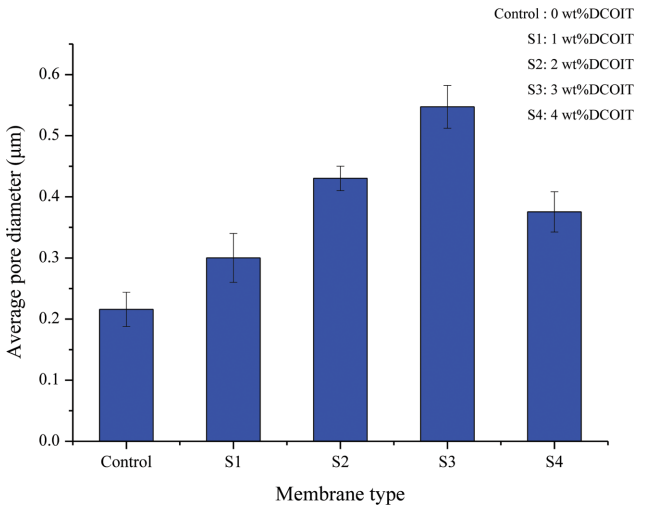

Fig. 4. Effects of different DCOIT contents on average pore diameter of the membranes.

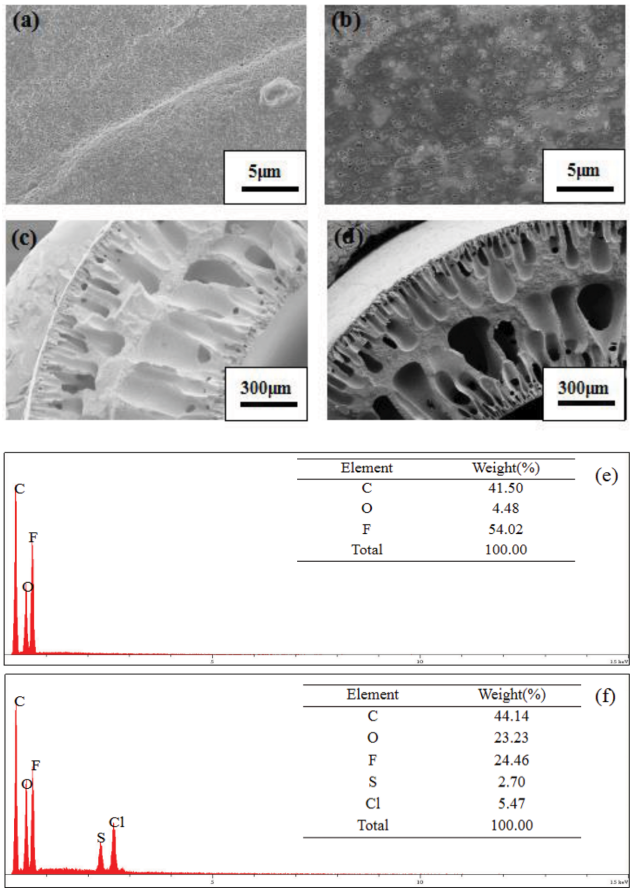

Fig. 5. SEM and EDS images of the prepared membranes: (a) The surface SEM images of 0 wt% DCOIT membrane, (b) the surface SEM images of 3 wt% DCOIT membrane, (c) the cross-sectional SEM images of 0 wt% DCOIT membrane, (d) the cross-sectional SEM images of 3 wt% DCOIT membrane, (e) EDS of 0 wt% DCOIT membrane, (f) EDS of 3 wt% DCOIT membrane.

characteristic elements, which distinguished the PVDF-DCOIT hollow fiber membrane from control group without DCOIT. EDS line spectra across the surface of the membrane samples was presented in Fig. 5(e), (f). The membrane with 3 wt% DCOIT showed clear signals for the presence of a steady sulfur and chlorine element. The ratio of sulfur and chlorine element in total weight (%) on the surface of 3 wt% DCOIT membrane accounted for 2.7% and 5.5%, respectively (Fig. 5(f)). The ratio was nearly 1 : 2, which was in accordance with the structure and additive amount of the DCOIT. Hence, DCOIT mixed evenly with casting solution could be proved and kept activity in the PVDF membrane materials.

The surface roughness of the prepared membranes was measured by atomic force microscopy (AFM). As shown in AFM images of Fig. 6(a)-(d), the brightest areas indicated the highest peaks of the surface and the darkest areas represented the lowest valleys or pores [36,37]. The surface roughness of 0 wt% DCOIT membrane was significantly higher than that of the membranes with 3 wt% DCOIT. According to Fig. 6(e), the average roughness (S_a) of 0 wt% DCOIT membrane and 3 wt% DCOIT membrane were 81.8 nm and 16.4 nm, respectively. The root mean square of the Z data (S_q) were 102.2 nm and 20.5 nm. And the average difference between the highest peaks and the lowest valleys relative to the plane (S_z) were 664.9 nm and 128.9 nm. The surface of the 0 wt% DCOIT membranes was obviously rougher than that of 3 wt% DCOIT membranes, which showed the smoother surface of membrane due to the better compatibility between the DCOIT and mem-

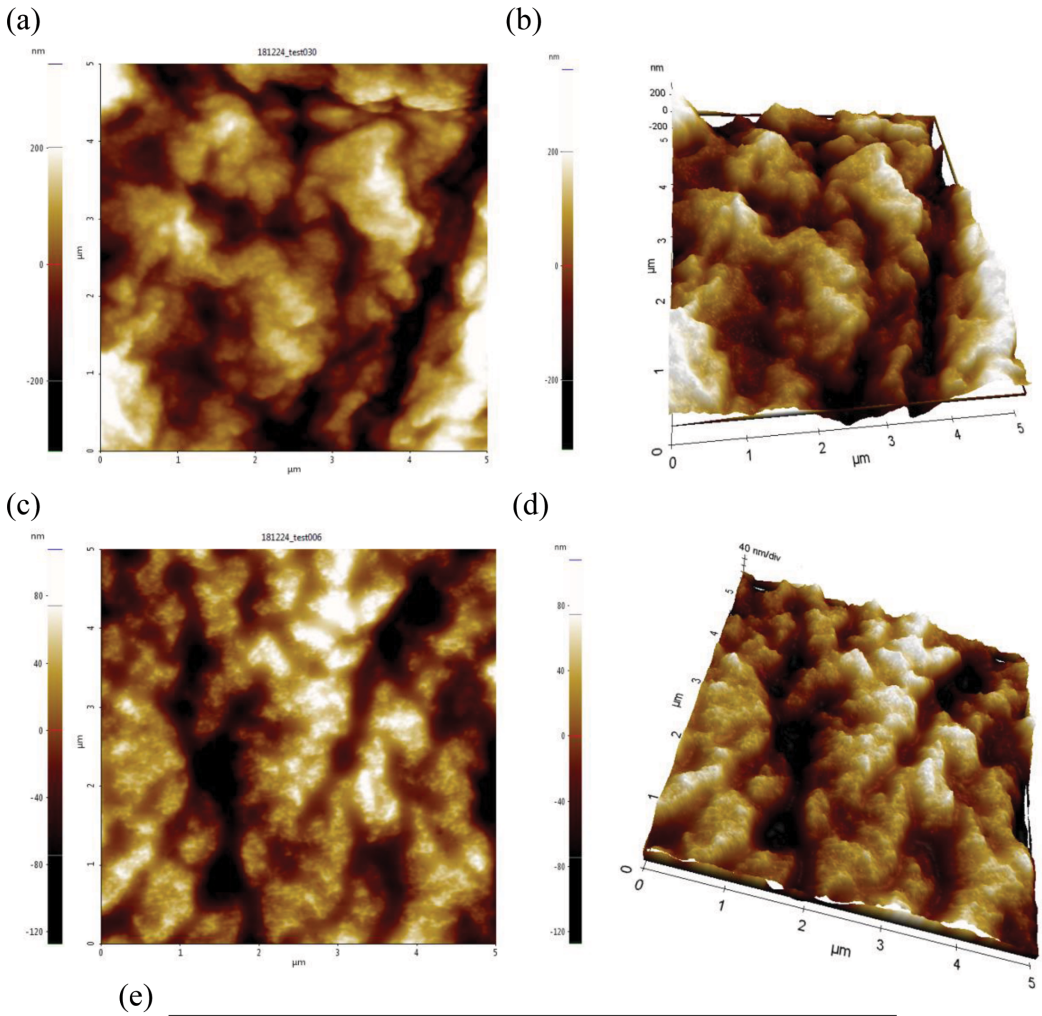

(e)

Membrane	Surface roughness parameters		
	S_a (nm)	S_q (nm)	S_z (nm)
0 wt% DCOIT	81.8	102.2	664.9
3 wt% DCOIT	16.4	20.5	128.9

Fig. 6. AFM images of the prepared membranes: (a) The two-dimensional images of 0 wt% DCOIT membrane, (b) the three-dimensional images of 0 wt% DCOIT membrane, (c) the two-dimensional images images of 3 wt% DCOIT membrane, (d) the three-dimensional images of 3 wt% DCOIT membrane, (e) surface roughness parameters of 0 wt% DCOIT membrane and 3 wt% DCOIT membrane resulted from analyzing AFM images.

brane material.

4. Antifouling Experiments against Model Foulants of Organic Matters

Antifouling experiments of the prepared membranes were conducted with the dead-end filtration device in 1 g/L bull serum albumin (BSA), 1 g/L sodium alginate (SA) and 1 g/L humic acid (HA) solution [9,38]. As shown in Fig. 7(a), the flux of the prepared membranes by filtrating BSA solution had continuous decline, since BSA molecules (about 67 kDa, for Stokes radius of 3.5 nm) are easier to be filled into membrane pores and form the pore blocking [39]. However, the flux variation of 3 wt% DCOIT membrane by filtrating 1 g/L BSA solution reduced slower (81.42%) than that of PVDF membrane without DCOIT (64.6%). As shown in Fig. 7(b), the flux of the membranes was significantly decreased by filtrating 1 g/L SA solution due to the formation of gel layer inside the pore channels after the SA molecules (120-190 kDa, for Stoke radius 0.03-0.04 μm) adsorbed on the pore wall [25]. But the flux variation of 3 wt% DCOIT membrane (54.3%) was still better than that of 0 wt% DCOIT membrane (24.72%) filtrated by filtrating SA solution. According to the conventional blocking mechanism, the HA molecules are initially adhered on the pore wall due to smaller particle size of HA molecules (10-50 kDa, for Stoke radius 3-7 nm) than membrane pores [40]. In fact, larger molecules were formed by the aggregation effect of HA molecules and then created cake blocking rather than absorbing on the membrane walls [41]. Fig. 7(c) depicted that the flux of the membranes with 3 wt% DCOIT (163.81 $L \cdot m^{-2} \cdot h^{-1} \cdot bar^{-1}$) had the sustained decline (50.5%) by filtrating 1 g/L HA solution, since a denser cake was formed on the membrane surface, especially in dead-end filtration, while the flux variation rate of the membrane without DCOIT was 29%. Therefore, the flux and its reduction rate of 3 wt% DCOIT membranes in DOM solution were both better than that of the PVDF membrane without DCOIT.

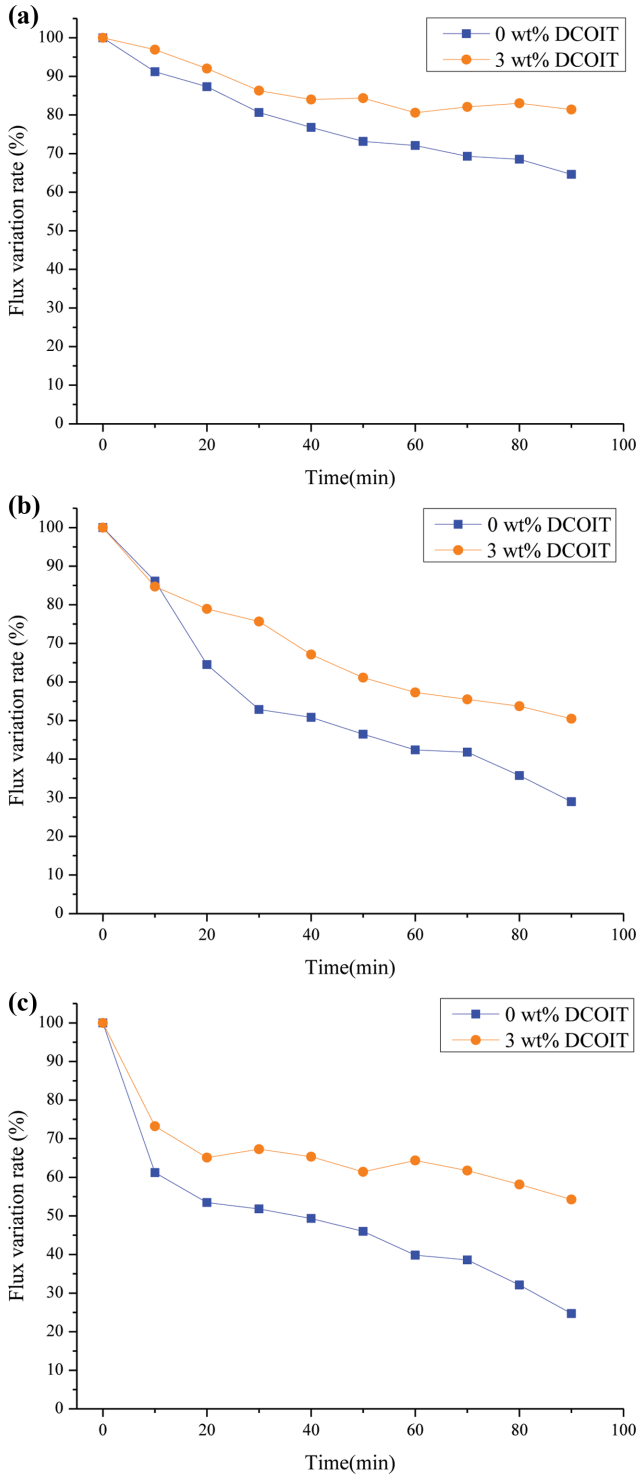

Fig. 7. The flux variation of the DCOIT blended PVDF membranes with filtrating different model pollutants: (a) 1 g/L bull serum albumin, (b) 1 g/L sodium alginate, (c) 1 g/L humic acid.

5. Antifouling Experiments with the Dead-end Filtration in Anaerobic Bioreactors

Besides organic pollutants, another vital membrane contamination is microbial fouling. During the operation of the membrane bioreactors, the active sludge cells were moved to the membrane surface and formed the cake layer owing to their large specific surface areas and adsorption of extracellular polymeric substances (EPS) [27,42]. With the accumulation of cake layer, flux of the prepared membrane will be significantly reduced. Conversely, the TMP was sharply increased. Meanwhile, EPS will also cause pore blockage and organic adsorption of the membrane due to their smaller particle sizes aggravating membrane pollution. The fouling caused by the microbial in anaerobic bioreactors (1 g/L MLSS) was analyzed via the water permeability and their flux variation rates. According to Fig. 8, the water flux of the prepared membranes in the anaerobic sluges was rapidly decreased. Relatively, the flux of the membranes without DCOIT was reduced faster than that of the membrane with 3 wt% DCOIT during the whole operation. DCOIT is an environmental-friendly and broad-spectrum antifouling agent which could be slowly released to kill the microorganisms attached to the membrane surface [9]. At the same time, membrane washing was carried out for 30 min after the filtration of 8 hours in order to alleviate microbial adhesion on the membrane surface. The flux reduction rate of the membrane with 3 wt% DCOIT was evidently slower than the control group which showed 3 wt% DCOIT membrane had better fouling resistance. Meanwhile, in the first, second and third stage, the flux variations of 3 wt% DCOIT membranes were 59.4%, 47.8% and 46.0%, respectively. However, the flux vari-

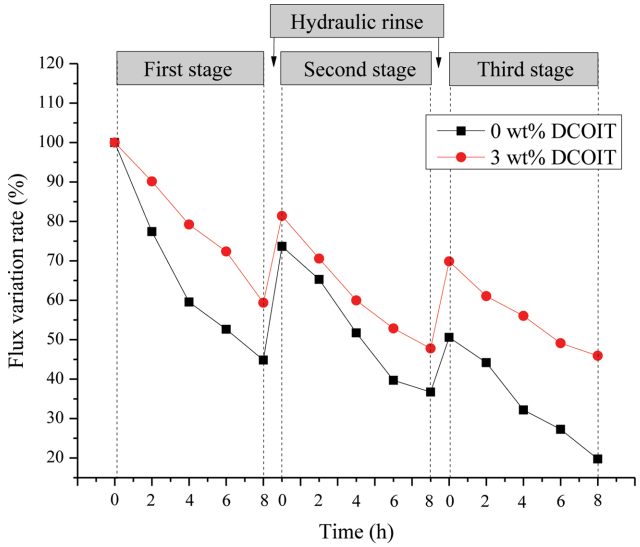

Fig. 8. Water flux variation of the prepared membranes in anaerobic batch bioreactors (membrane rinse every 8 hours).

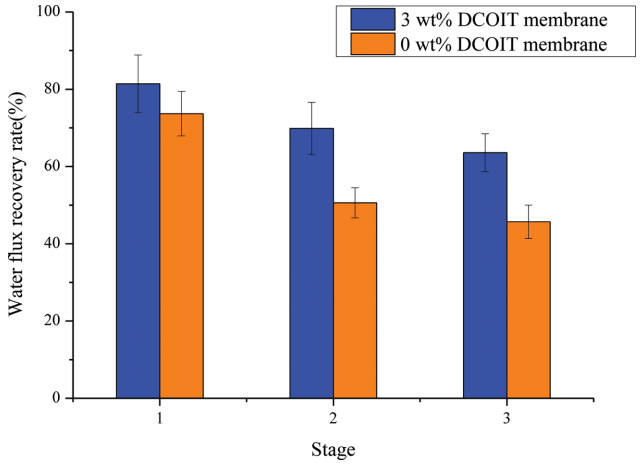

Fig. 9. Water flux recovery of the prepared membranes in dead-end filtration in three stages for 24 h.

ations of membranes without DCOIT were 44.8%, 36.7% and 19.8%, respectively. And the gap between two membrane modules was increased with the increase of time which evidently indicated that the new membranes had better controlling of microbial adhesion. The phenomenon should be ascribed to the good sterilization and antifouling of DCOIT, which decreased microbial adhesion on membrane surface. Furthermore, water flux recovery of the prepared membranes in dead-end filtration for 24 h was depicted in Fig. 9. The total flux recovery efficiency of 3 wt% DCOIT membrane was also higher than that of membrane without DCOIT via dead-end filtration devices in three stages for 24 h which manifested that 3 wt% DCOIT membranes had better antimicrobial activity and longer service life than control group. The variation tendency of flux recovery ratio was also consistent with membranes' hydrophilicity. Hydrophilic membrane surface were beneficial to adsorb H_2O molecules and promote the formation of water layer [26,31], which alleviated the adsorption of organic or microbial foulants. Flux recovery of the membrane with 3 wt% DCOIT was higher than membrane without DCOIT, which showed better biofoluing-resistance performance than PVDF membrane without DCOIT.

In conclusion, DCOIT as an active fungicide could increase the compatibility of N, N-dimethylformamide (DMF) (hydrophilic and polar substance), glycerol (hydrophilic and polar substance) and PVDF (non-polar substance) [43]. And better compatibility of hydrophilic materials and PVDF endowed membrane better anti-fouling performance. Moreover, DCOIT also reduced some microbial fouling in a degree, which showed the superiority of the novel membrane compared to normal membranes.

CONCLUSIONS

In this work, the novel PVDF-DCOIT hollow fiber membrane was prepared by conventional NIPS method. As the additive, DCOIT evidently enhanced the general filtration and antifouling performance of the composite membrane. The water contact angle (63.35°), the pure water flux (393.86 $L \cdot m^{-2} \cdot h^{-1} \cdot bar^{-1}$), overall porosity (84.68%) and mean pore diameter (0.54 μm) were markedly improved than those of 0 wt% DCOIT membrane. SEM images revealed better finger-like porous structure of the PVDF-DCOIT composite membranes. And AFM images showed smoother surface of composite membranes to alleviate the membrane fouling. In antifouling experiments, the flux variation rate of membranes with 3 wt% DCOIT filtrated in bull serum albumin, sodium alginate and humic acid solution were 81.42%, 54.25%, 50.5%, while membrane without DCOIT were 64.6%, 24.72% and 29%, respectively. And the flux variations of 3 wt% DCOIT membranes were 59.4%, 47.8% and 46.0%, respectively in three stages while the flux variations of membranes without DCOIT were 44.8%, 36.7% and 19.8%, respectively. The results showed that DCOIT could be an excellent membrane additive which would provide an effective way to enhance membrane antifouling properties by physical blending with the antifouling booster biocide DCOIT.

ACKNOWLEDGEMENT

Thanks for the financial support by the National Natural Science Foundation of China (No. 21677026), the Fundamental Research Funds for the Central Universities (DUT17LAB15) and the Programme of Introducing Talents of Discipline to Universities (B13012).

REFERENCES

1. K. Xiao, S. Liang, X. Wang, C. Chen and X. Huang, *Bioresour. Technol.*, **271**, 473 (2019).
2. M. Ping, X. Zhang, M. Liu, Z. Wu and Z. Wang, *J. Membr. Sci.*, **570**, 286 (2019).
3. M. Bagheri and S. A. Mirbagheri, *Bioresour. Technol.*, **258**, 318 (2018).
4. X. Zhao, R. Zhang, Y. Liu, M. He, Y. Su, C. Gao and Z. Jiang, *J. Membr. Sci.*, **551**, 145 (2018).
5. P. Li, L. Liu, J. Wu, R. Cheng, L. Shi, X. Zheng and Z. Zhang, *Sci. Total Environ.*, **647**, 627 (2019).
6. F. Meng, S.-R. Chae, A. Drews, M. Kraume, H.-S. Shin and F

Yang, *Water Res*., **43**, 1489 (2009).
7. X. Fu, T. Maruyama, T. Sotani and T. Matsuyama. *J. Membr. Sci*., **320**, 483 (2008).
8. T. Nguyen, F. Roddick and L. H. Fan, *Membranes*, **2**, 804 (2012).
9. R. Zhang, Y. Liu, M. He, Y. Su, X. Zhao, M. Elimelech and Z. Jiang, *Chem. Soc. Rev*., **45**, 5888 (2016).
10. F. Liu, N. A. Hashim, Y. Liu, M. R. M. Abed and K. Li, *J. Membr. Sci*., **375**, 1 (2011).
11. M. Bagheri and S. A. Mirbagheri, *Bioresour. Technol*., **258**, 318 (2018).
12. K. Gao, Y. Su, L. Zhou, M. He, R. Zhang, Y. Liu and Z. Jiang, *J. Membr. Sci*., **548**, 621 (2018).
13. M. S. Mauter, Y. Wang, K. C. Okemgbo, C. O. Osuji, E. P. Giannelis and M. Elimelech, *ACS Appl. Mater. Interfaces*, **3**, 2861 (2011).
14. M. Ben-Sasson, X. Lu, E. Bar-Zeev, K. R. Zodrow, S. Nejati, G. Qi, E. P. Giannelis and M. Elimelech, *Water Res*., **62**, 260 (2014).
15. M. Ben-Sasson, K. R. Zodrow, Q. Genggeng, Y. Kang, E. P. Giannelis and M. Elimelech, *Environ. Sci. Technol*., **48**, 384 (2014).
16. S. S. Caldas, B. M. Soares, F. Abreu, I. B. Castro, G. Fillmann and E. G. Primel, *Environ. Sci. Pollut. Res*., **25**, 7553 (2018).
17. R. J. C. A. Steen, F. Ariese, B. Hattum, J. Jacobsen and A. Jacobson, *Chemosphere*, **57**, 513 (2004).
18. A. H. Jacobson and G. L. Willingham, *Sci. Total Environ*., **258**, 103 (2000).
19. I. K. Konstantinou and T. A. Albanis, *Environ. Int*., **30**, 235 (2004).
20. A. Behboudi, Y. Jafarzadeh and R. Yegani, *J. Environ. Chem. Eng*., **6**, 1764 (2018).
21. G.-D. Kang and Y. Cao, *J. Membr. Sci*., **463**, 145 (2014).
22. J.-K. Jiang, Y. Mu and H.-Q. Yu, *J. Colloid Interface Sci*., **535**, 318 (2019).
23. Y. Yang, S. Qiao, R. Jin, J. Zhou and X. Quan, *Korean J. Chem. Eng*., **35**, 964 (2018).
24. X. Zhao and C. Liu, *J. Membr. Sci*., **515**, 29 (2016).
25. Y. Xi, M. Huang and X. Luo, *Appl. Surf. Sci*., **467**, 135 (2019).
26. X. Fu, T. Maruyama, T. Sotani and H. Matsuyama, *J. Membr. Sci*., **320**, 483 (2008).
27. G.-P. Sheng, H.-Q. Yu and X.-Y. Li, *Biotechnol. Adv*., **28**, 882 (2010).
28. Y. Yang, S. Qiao, R. Jin, J. Zhou and X. Quan, *J. Membr. Sci*., **553**, 54 (2018).
29. S. Zinadini, A. A. Zinatizadeh, M. Rahimi, V. Vatanpour and H. Zangeneh, *J. Membr. Sci*., **453**, 292 (2014).
30. Y. Sun, K. Zhu, B. Khan, X. Du, L. Hou, S. Zhao, P. Li, S. Liu, P. Song and H. Zhang, *Mater. Sci. Eng*., **301**, 012031 (2018).
31. M. L. Yeow, Y. T. Liu and K. Li, *J. Appl. Polym. Sci*., **92**, 1782 (2004).
32. X. Chang, Z. Wang, S. Quan, Y. Xu, Z. Jiang and L. Shao, *Appl. Surf. Sci*., **316**, 537 (2014).
33. L. Y. Lafreniere, F. D. F. Talbot, T. Matsuura and S. Sourirajan, *Ind. Eng. Chem. Res*., **26**, 2385 (1987).
34. H.-H. Lin, Y.-H. Tang, H. Matsuyama and X.-L. Wang, *J. Membr. Sci*., **548**, 288 (2018).
35. S. Mohsenpour and A. Khosravanian, *J. Appl. Polym. Sci*., **135**, 46225 (2008).
36. E. Koh and Y. T. Lee, *J. Ind. Eng. Chem*., **47**, 260 (2017).
37. Q. Wang, Z Wang, J. Zhang, J. Wang and Z. Wu, *RSC Adv*., **4**, 43590 (2014).
38. Q. Wu, G.-E. Chen, W.-G. Sun, Z.-L. Xu, Y.-F. Kong, X.-P. Zheng and S.-J. Xu, *Chem. Eng. J*., **313**, 450 (2017).
39. Z. Wang, Y. Song, M. Liu, J. Yao, Y. Wang, Z. Hu and Z. Li, *Desalination*, **249**, 1380 (2009).
40. Z. Wang, Y. Wan, P. Xie, A. Zhou, J. Ding, J. Wang, L. Zhang, S. Wang and T. C. Zhang, *Chemosphere*, **214**, 136 (2019).
41. M. H. Le, K.-J. Kim and A. Jang, *KSCE J. Civ. Eng*., **22**, 4814 (2018).
42. D. C. Banti, P. Samaras, C. Tsioptsias, A. Zouboulis and M. Mitrakas, *Sep. Purif. Technol*., **202**, 119 (2018).
43. J. Feng, H. Zhang, H. He, X. Huang and Q. Shi, *BioResources*, **11**, 4069 (2016).